

Turbulent intermittency and Euler similarity solutions

Daniel P. Lathrop

Department of Physics

Institute for Research in Electronics and Applied Physics

Institute for Physical Sciences and Technology

University of Maryland, College Park, MD 20742

Self-similar Euler singularities may be useful for understanding some aspects of Navier-Stokes turbulence. Here, a causal explanation for intermittency is given, based on the control of the sudden growth of the gradients by the Euler equations. This explanation uses certain Euler solutions as intermediate asymptotics in Navier-Stokes turbulence [1] – controlling the dynamics over a limited spatial and temporal domain. These arise from an analysis of similarity equations, previously discussed by Pelz and Green [2], which yield experimentally testable predictions. Three main points are presented here: scalings of suitable characteristic lengths with time from a critical time $l \sim (t_0 - t)^\alpha$, $\alpha > 1$, a discussion of invariant sets of the similarity equations that result, and a discussion of cutoff mechanisms. The value $\alpha = 3/2$ appears to correspond to Kolmogorov scaling for turbulence. Some limited experimental evidence is presented from Eulerian gradient measurements at the Kolmogorov scale showing $1 < \alpha < 3$ values. Much testing is necessary to ascertain the final usefulness and validity of these ideas, as several conceptual obstacles remain.

1 Introduction

Turbulent flows of liquids and gases occur in a host of natural and engineering phenomena. A detailed understanding of atmospheric flows on Earth and the planets, predictive design for industrial equipment, and understanding of the processes within the liquid cores of planets all rely on an understanding of turbulence. One might naively think this an easy task, given that the governing equations are well known (i.e., the family of equations stemming from the Navier-Stokes equations with appropriate body forces). That understanding is hampered by the inherent nature of turbulence itself, where the velocity field is rough and velocity gradients are intermittent. Phenomenological considerations of Richardson and Kolmogorov have been very fruitful [3, 4], but have also left deep holes in our understanding of the intermittent nature of turbulence[5]. By intermittency, I mean a host of interlocking observations that the basic observables in turbulent flow; the vorticity, dissipation, helicity, acceleration, and their ability to effect advected scalar and vector fields (concentration or perhaps magnetic fields) all show abnormal statistics. As one example, in experiments one can observe accelerations hundreds times the means, lying 30 standard deviations from those means [6, 7], or observe the dissipation locally becoming one hundred times its average value [8, 9, 10]. The probability distributions for these observable then show far from Gaussian statistics with long tails. These types of gradient or time derivative concentrations appear local in space and time. Recent results of Gibbon and Doering suggest that the time intervals where singularities are possible become more localized as the Reynolds number increases [11].

There is little in the phenomenological picture of a cascade of energy to smaller scale (envisioned in wavenumber space) to explain intense events. The framework discussed here is an attempt to explain these observations, although it is as yet a hypothetical explanation. Rather than attempting a phenomenological explanation, instead I seek a causal explanation rooted in the known equations of motion and the relevant forces.

This is a non-statistical approach, but with the need to ultimately explain the observed statistics. First, I argue that the viscous forces are not responsible for the sudden growth locally of gradients, and that in

this context, during the growth, one should consider the viscous forces irrelevant. This limits our scope to the growth phase of these events, and lands us in the context of the Euler equations. Solutions to the Euler equations may explain the sudden growth in the gradients and time derivatives in the context of an intermediate asymptotic [1]. These solutions will be locally relevant for only a range in times, nearby the sudden collapse, but limited to times before viscosity, or perhaps cavitation, act to limit the strength of these near-singularities. As an example, one can look to the Burgers equation [12]. There, negative slopes tend to collapse to form shocks, but the gradients are limited by the action of viscosity. In the case when the viscosity is quite small, there is a substantial range in time where the gradient value at the location of minimum gradient is approximately governed by the inviscid Burgers equations, with the gradients growing as predicted, i.e. inverse in time from a critical time.

What is unlikely to be understood through this exercise are the important long lived vortices so many have remarked on [40], which form an independent, but perhaps causally connected part of turbulent phenomena. Remarks on the connection between long lived vortex filaments and the local collapse of gradients studied here are given in the conclusion.

When entering the study of gradient focusing and local intermittent events in turbulence, one treads on the long worn and active path of singularities in Navier-Stokes and Euler equations [27, 28, 15, 29, 33, 34, 36, 37, 38, 39]. Although these studies are conceptually related, I view the Euler solutions discussed here (which are singularities of the Euler equations) as merely intermediate asymptotics for Navier-Stokes, as remarked earlier, and not observable singularities of viscous fluid flow. Many previous studies have concentrated on the Leray scaling $\alpha = 1/2$ [13, 2] or on the case where a co-collapsing sphere shows energy conservation $\alpha = 2/5$ [14]. At least one simulation of R.M. Kerr has shown some evidence for $\alpha = 1$ behavior [15]. I restrict my attention to the case (described later) of $\alpha > 1$ so that, as observed in turbulence, the velocities are not growing abnormally large. In many turbulent flows the probability distribution of the velocity is close to Gaussian, while the gradients are intermittent.

Whether or not there are singularities in Navier-Stokes solutions is perhaps of little practical consequence – extra phenomena such as dilations, cavitation or extreme rarity render them of little relevance. One should not mistake the irrelevance of singularities of the Navier-Stokes equations for an argument for the same for Euler singularities. Here, I’m proceeding based on the premise that *the causal structure of Euler singularities is the underlying cause of intermittency in Navier-Stokes turbulence*, even if they are capped by viscosity or other extra constraints.

While the following calculations and observations are presented with the hope of better understanding Navier-Stokes turbulence, their final utility is yet unknown. Nevertheless, because of the possibility of their importance, it seems useful to present them.

2 Similarity methods

There have been significant successes in understanding singularities and self-focusing in strongly nonlinear physical systems using similarity methods [1, 17, 18, 19, 20]. Our previous work on the collapse of waves and the production of jets on a free surface illustrates the utility of similarity techniques in allowing analytical and numerical progress on systems not otherwise amenable to analysis [21]. While there is no guarantee of the success of this approach for Euler collapse, proceeding with this hope may lead to new insight. Observe that in local gradient collapse the length scales become small as one approaches maximum focusing. In what follows I will assume that useful information can be obtained by consideration of the hypotheses that the length scales in all directions behave equally, and that the functional form is a power law in time. Regarding the first hypothesis, one might say that the different directions may have trouble behaving in different manners as they are constantly effecting each other and being mixed by motions and rotations. This argument, however, is hardly compelling. One might also argue that the relevant equations balance

linear and nonlinear terms, so power-law time dependences may arise. This, however, is not necessary and depends on the algebraic form of these balances. There might be collapse events of more complicated forms; understanding their analytical structure may be much more difficult.

Beginning with the Euler equations for incompressible flow:

$$\partial_t \vec{v} + (\vec{v} \cdot \vec{\nabla}) \vec{v} + \frac{1}{\rho} \vec{\nabla} P = 0 \quad (1)$$

$$\vec{\nabla} \cdot \vec{v} = 0, \quad (2)$$

one can apply the above assumptions to form an intelligent guess for the form of the solutions:

$$\vec{v}(\vec{x}, t) = v^* \left(\frac{t_o - t}{t^*} \right)^{\alpha-1} \vec{G} \left(\frac{\vec{x}}{L^*} \left(\frac{t^*}{t_o - t} \right)^\alpha \right) \quad (3)$$

$$P(\vec{x}, t) = \rho (v^*)^2 \left(\frac{t_o - t}{t^*} \right)^{2\alpha-2} \Pi \left(\frac{\vec{x}}{L^*} \left(\frac{t^*}{t_o - t} \right)^\alpha \right) \quad (4)$$

Here various quantities are made dimensionless using some characteristic large scale L^* , velocity scale v^* , and time scale $t^* = L^*/v^*$, as would be natural in the context of a shear flow. One can then seek solutions for the time independent similarity functions \vec{G} and Π . The above ansatz assumes all lengths scale as $l \sim (t_o - t)^\alpha$, velocities as $v \sim (t_o - t)^{\alpha-1}$. It is important to require that $\alpha \geq 1$ in order that the velocities remain bounded as we approach t_o from below. By defining a scaled coordinate \vec{r} and a scaled gradient

$$\vec{r} = \frac{\vec{x}}{L^*} \left(\frac{t^*}{t_o - t} \right)^\alpha \quad (5)$$

$$\hat{\nabla} = \left(\frac{t_o - t}{t^*} \right)^\alpha L^* \vec{\nabla} \quad (6)$$

one can eliminate time dependence from the Euler equations and obtain what are referred to as similarity equations

$$(1 - \alpha) \vec{G} + \alpha (\vec{r} \cdot \hat{\nabla}) \vec{G} + (\vec{G} \cdot \hat{\nabla}) \vec{G} + \hat{\nabla} \Pi = 0, \quad (7)$$

$$\hat{\nabla} \cdot \vec{G} = 0. \quad (8)$$

Solutions to Eqs. 7 and 8 correspond to solutions to the original Euler equations. Symmetries of the Euler equations may be used to generate further solutions associated with the similarity ansatz. The time or spatial origin of the solutions may be shifted, and one may also add a constant velocity.

The solutions to Eq. 7 are assumed to be smooth – they represent solutions which retain their smoothness up to the critical time t_o , and loose it by the length scales limiting to zero. At that critical time the solution remains smooth at all locations (governed by the far field of Eq. 7) except at the origin, where the gradients become unbounded. Pelz and Green [2] have examined the stability properties of these solutions. Here I present new results and discussion on the form of the solutions of Eq. 7, their correspondence to Lagrangian dynamics, viscous cutoff mechanisms, and their relationship to turbulence with Kolmogorov statistics.

I examine the similarity equations progressively in one, two and three dimensions, in order to better understand their function and utility.

3 One dimensional similarity equations

In one dimension, one neglects the requirement of incompressibility and drops the pressure term in Eq. 7. In this case:

$$(1 - \alpha)G + \alpha x \partial_x G + G \partial_x G = 0. \quad (9)$$

This equation has several families of implicit analytical solutions [22], only one of which is relevant here:

$$x = -G + aG^{\alpha/(\alpha-1)} \quad (10)$$

The far field (i.e., large $|x|$) limit of Eq. 10 is $G = x^{1-1/\alpha}$. This similarity solution gives the generic formation of the first shock in the inviscid Burgers equation, and accurately describes the formation of a near-shock in the diffusive case, when the diffusion is small. In particular, Burgers equation is unstable where the slope has a maximum negative value, the magnitude of the slope following a characteristic diverges as $(t_o - t)^{-1}$ for a time until the diffusive cutoff takes over. The value $\alpha = 3/2$ is generically seen, due to a curious reason, and leading to a $G \sim |x - x_o|^{1/3}$ far field. The location for the characteristic which sees the first shock in the inviscid case is the most negative slope in the initial condition. Generically, the second derivative will vanish there; locally the curve will be dominated by the linear and cubic terms. These cubic terms yield, in the confluence of characteristics in the shock, a functional form at the time of the shock $u = u_o + v_*|(x - x_o)/L^*|^{1/3}$. The probability distribution of negative gradients in randomly forced Burgers turbulence is governed by these pre-shocks [23].

4 Two dimensional similarity equations

The situation in two dimensions is quite different. Due to the simple advection of vorticity in two dimensions [24] – the vorticity remains bounded and no similarity solutions exist. However, examining this in more detail will assist in understanding the three-dimensional case.

In two dimensions, the vorticity vector lies normal to the plain of motion. Due to this, there are no gradients of the vorticity along the direction of the vorticity, and one can write the vorticity similarity equation (curl of Eq. 7) as:

$$\omega + \alpha(\vec{r} \cdot \hat{\nabla})\omega + (\vec{G} \cdot \hat{\nabla})\omega = 0 \quad (11)$$

I can demonstrate that these equations have no solutions using several observations. First, define the associated vector field $\vec{H} = \alpha\vec{r} + \vec{G}$. This field is used to rewrite the vorticity similarity equations in two dimensions as:

$$\omega + (\vec{H} \cdot \hat{\nabla})\omega = 0 \quad (12)$$

It is useful to define the dynamical system:

$$\frac{d\vec{r}}{ds} = \vec{H} \quad (13)$$

which yields characteristics for the vorticity. In terms of the trajectory $\vec{r}(s)$ one can write the vorticity equation along these characteristics as

$$\frac{d\omega}{ds} = -\omega. \quad (14)$$

The dynamical system for $\vec{r}(s)$ is everywhere expanding, as $\hat{\nabla} \cdot \vec{H} = 2\alpha$ and α is positive. Nearly all trajectories starting out near the origin escape to infinity. Due to the (assumed) smoothness of the dynamical

system, Eq. 13, there must be an invariant set near the origin which does not escape. As this calculation is restricted to two dimensions, the possible invariant sets (by the Poincare-Bendixon theorem [25]) may be fixed points or closed orbits. Along any characteristic $\vec{r}(s)$ the vorticity must be $\omega(s) = \omega(0)e^{-s}$. At fixed points, by definition, $\vec{H} = 0$, giving $\omega = 0$ from Eq. 12 at those points. For closed orbits, the vorticity ω must also be zero so that after going around one orbit it returns to its original value. Points starting nearby the closed orbits or fixed points escape to large radius. As their initial vorticity must be zero, as they move out from near the origin their vorticity remains zero. From this one can understand that the vorticity is zero everywhere in the plain. The far field (large $|\vec{x}|$) solution for \vec{G} must have a dependence rising like $r^{(\alpha-1)/\alpha}$, where the first two terms of Eq. 7 are dominant. As the vorticity is zero (i.e., $\hat{\nabla} \times \vec{G} = 0$), the vector field $\vec{G} = \hat{\nabla}\phi$ must be a gradient field with $\nabla^2\phi = 0$. The far field dependence is incompatible with a smooth Harmonic function ϕ which must have an integer n far field dependence r^n . The far field exponent $(\alpha-1)/\alpha$ is not an integer for all cases of interest $\alpha > 1$. Thus, the only solution to the similarity equations in two dimensions are $G = \omega = 0$. Another proof is also possible using integral methods [26].

5 Three dimensional similarity equations - Lagrangian dynamics

The flow generated by \vec{H} is also of considerable use in understanding the three dimensional case. Trajectories of Eq. 13 are directly associated with particle trajectories $\vec{x}(t)$ in lab coordinates. The invariant sets are especially important and correspond to trajectories which undergo the most singular Lagrangian motions. Trajectories in the laboratory frame follow a path $d\vec{x}/dt = \vec{v}$; this equation is equivalent to Eq. 13 under the identifications of $s = -\ln[(t_o - t)/t^*]$ and Eq. 5 for \vec{r} . The correspondence between these different quantities is summarized in the diagram:

$$\begin{array}{ccccc}
 & t & \xrightarrow{\vec{v}} & \vec{x} & \\
 -\ln[(t_o - t)/t^*] & \downarrow & & \downarrow & \vec{x}[t^*/(t_o - t)]^\alpha/L^* \\
 & s & \xrightarrow{\vec{H}} & \vec{r} &
 \end{array} \tag{15}$$

Note as $(t_o - t) \rightarrow 0$, that $s \rightarrow \infty$. As the flow generated by \vec{H} has divergence everywhere positive ($\hat{\nabla} \cdot \vec{H} = 3\alpha$), trajectories all flow outward toward large radius, and there must be repelling invariant sets in the vicinity of the origin (assuming of course that the similarity solution is smooth and exists!). Several types of invariant sets are possible: fixed points, closed orbits, or perhaps strange saddles¹. Which type of invariant set will be determined by the precise form of the outer solution. Assuming these solutions exist, and pending a numerical solution, it is useful to explore the consequences of these invariant sets. Fixed points of the dynamical system Eq. 13 are defined by $\vec{H} = 0$; we label them \vec{r}^* . These points have a number of properties and yield testable prediction for the Lagrangian motion. At points \vec{r}^* , one has that $\alpha\vec{r} = -\vec{G} = -\hat{\nabla}\Pi$ from the definition of \vec{H} and the similarity equation (Eq. 7) with $\vec{H} = 0$.

We can see why the non-existence proof for two dimensions fails in three by examining the vorticity equation in three dimensions (the curl of the similarity Eq. 7):

$$\vec{\omega} + (\vec{H} \cdot \hat{\nabla})\vec{\omega} = (\vec{\omega} \cdot \hat{\nabla})\vec{G}. \tag{16}$$

Rather than the vorticity being zero at the fixed points of Eq. 13, the vorticity must be a eigenvector of the gradient matrix with unit eigenvalue $M\vec{\omega} = \vec{\omega}$. Although the 2-D non-existence does not carry over to 3-D, I have yet been unable to show existence directly, numerics may give some evidence in future work.

¹2-tori are excluded, since their interior volumes would be invariant, contradicting $\hat{\nabla} \cdot \vec{H} = 3\alpha > 0$ which implies that all volumes grow exponentially as $\exp(3\alpha s)$ following the flow defined by Eq. 13.

From the equivolency of flows of \vec{H} and Lagrangian trajectories, one can calculate the form for observables due to the fixed points and limit cycles of the similarity flow. For a fixed point \vec{r}^* transformed to laboratory coordinates the trajectory is $\vec{x} = L^*[(t_o - t)/t^*]^\alpha \vec{r}^* + \vec{v}_o t + \vec{x}_o$, where we have allowed for a background velocity and origin. The Lagrangian velocity would be $\dot{\vec{x}} = -\alpha L^*[(t_o - t)/t^*]^{\alpha-1} \vec{r}^*/t^* + \vec{v}_o$; acceleration would be $\ddot{\vec{x}} = \alpha(\alpha - 1)L^*(t_o - t)^{\alpha-2} \vec{r}^*/(t^*)^2$. This acceleration diverges at the critical time, clearly in need of a cutoff due to viscosity or other physical intervention. These forms, as intermediate asymptotics are testable predictions for Lagrangian experiments and numerics – are events observed which hold such forms?

In the case of an invariant cycle in the flow of \vec{H} one obtains a different type of motion. This rotating motion in similarity coordinates, with some characteristic frequency in s , yields an accelerating chirp of spiraling motion. For simplicity, let's say some similarity coordinate has harmonic motion $r_1 = A \cos(\Omega s)$. Carried to laboratory coordinates the motion is

$$x_1 = AL^* \left(\frac{t_o - t}{t^*} \right)^\alpha \cos[\Omega \ln(\frac{t_o - t}{t^*})]. \quad (17)$$

The laboratory Lagrangian frequency thus rises as $(t_o - t)^{-1}$ while the radius collapses to zero as $(t_o - t)^\alpha$. Such motions may be related to the large accelerations observed in recent Lagrangian tracking experiments [6, 7], and may account partially for the extreme intermittency seen in the acceleration distributions. It is a likelihood that a clear understanding of the viscous cutoff is needed to fully account for such distributions; some aspects of the viscous cutoff are discussed in Sec. 8. These calculations give a plausible specific cause for extreme Lagrangian accelerations – which is independent of the intense long-lived vortices which form an alternative explanation for those observations.

6 Far field behavior

The large r behavior is particularly significant, as close to the critical time, the near field character has shrunk (in laboratory coordinates) into an insignificant volume, leaving a relatively large area displaying the far field behavior in its wake. For large r , one can calculate the behavior of three dimensional solutions of Eq. 7. Only the first and second terms are relevant, the nonlinear term and pressure are sub-dominant. In that case the resulting equation $(1 - \alpha)\vec{G} + \alpha(\vec{r} \cdot \hat{\nabla})\vec{G} = 0$ is analytically solvable:

$$\vec{G} = r^{(\alpha-1)/\alpha} \vec{f}(\theta, \phi) \quad (18)$$

for spherical coordinates r, θ, ϕ . The function \vec{f} is a general $S^2 \rightarrow \mathcal{R}^3$ vector field subject only to $\hat{\nabla} \cdot \vec{G} = 0$.

Thus observe that the far field radial dependence is fixed by α , while the angular dependence is general. It has been conjectured [30] that Eq. 7 has solutions for all admissible far field forms, while it is important to emphasize solutions (numerical or analytical) have not yet been found.

The far field behavior has particular significance if one hopes to use these solutions to understand turbulence. The far field solution when $\alpha = 3/2$, if applied in many events, would lead to velocity difference statistics associated with Kolmogorov scaling and the known scaling for the third order structure function. When $\alpha = 3/2$ the far field behaves as $\|\vec{G}\| \sim r^{1/3}$, which is retained in the lab frame velocity near the critical time. This connection in particular has been a motivation for seeking a connection between these Euler similarity solutions and Navier-Stokes turbulence. Why the $\alpha = 3/2$ case may be prevalent is precisely unknown, but discussed in the conclusion.

7 Near field behavior

One can learn about the structure of the gradients at the fixed points by examining the similarity equation. Taking the gradient of that equation, to obtain a matrix equation for $M = \partial_i G_j$, one obtains at the fixed

points $\vec{H} = 0$ that:

$$M + M^2 + \Pi_2 = 0. \quad (19)$$

This matrix Riccati equation is related to the quadratic nonlinearities in the Euler equations. Gibbon [31] has shown how quaternions can be used in this context to relate Euler equations and the equations of ideal magneto-hydrodynamics to a Schrödinger equation. Equation 20 yields nine constraints on the components of M and Π_2 . Rotating M into a form where the symmetric part is diagonal, and given that Π_2 is symmetric, there are eleven independent components between them. Solving Eq. 19 yields three types of solutions, each in two parameters. Further solutions come from permuting the axis in this form, or by rotations relaxing the diagonalization of the symmetric part of M .

$$M = \begin{pmatrix} a & 0 & 0 \\ 0 & b & 0 \\ 0 & 0 & -a-b \end{pmatrix} \quad (20)$$

$$\Pi_2 = \begin{pmatrix} a(a+1) & 0 & 0 \\ 0 & b(b+1) & 0 \\ 0 & 0 & (a+b)^2 - (a+b) \end{pmatrix}$$

$$M = \begin{pmatrix} 1 & 0 & 0 \\ 0 & a & f \\ 0 & f & -1-a \end{pmatrix} \quad (21)$$

$$\Pi_2 = \begin{pmatrix} 2 & 0 & 0 \\ 0 & a+a^2-f^2 & 0 \\ 0 & 0 & a+a^2-f^2 \end{pmatrix}$$

$$M = \begin{pmatrix} 1 & 0 & f \\ 0 & 1 & g \\ f & g & -2 \end{pmatrix} \quad (22)$$

$$\Pi_2 = \begin{pmatrix} 2-f^2 & -fg & 0 \\ -fg & 2-g^2 & 0 \\ 0 & 0 & 2-f^2-g^2 \end{pmatrix}$$

The gradient matrix at these fixed points gives rise to rapidly growing gradients in laboratory coordinates. At these points, taking the gradient of Eq. 3, yields:

$$\frac{\partial v_i}{\partial x_j} = M v^* \left(\frac{t_o - t}{t^*} \right)^{-1} \quad (23)$$

leading to the vorticity and strains all growing jointly and suddenly.

8 Viscous cutoff

One can obtain estimates for the small scale cutoff for these events by analyzing the relevant forces. For all events with $\alpha > 1$ viscosity will be relevant at some late time, where the length scales become small enough for the local Reynolds number to be of order unity. Comparing the inertial forces with viscous forces for the scaling ansatz, $(\vec{u} \cdot \vec{\nabla})\vec{u} < \nu \nabla^2 \vec{u}$ yields an expression for the time when (for smaller $(t_o - t)$) viscosity will be dominant. This happens when

$$\frac{t - t_o}{t^*} < (R^*)^{1/(1-2\alpha)}, \quad (24)$$

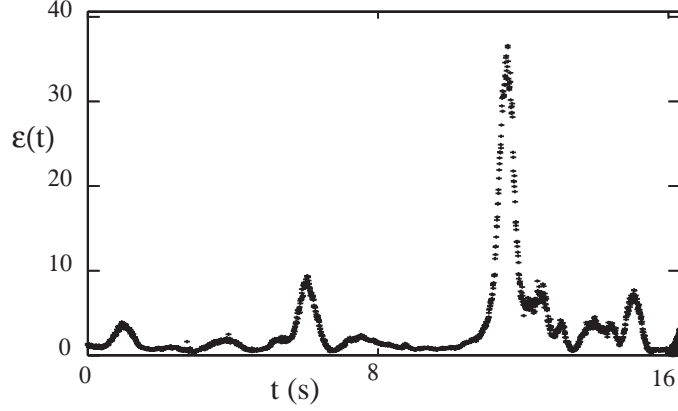


Figure 1: Time trace of the dissipation measured at the Kolmogorov scale in an oscillating grid experiment.

where $R^* = u^* L^* / \nu$. This leads to a definition of a crossover time t_k where the equality holds above. At the crossover time, the length scale is

$$l_k = L^* (R^*)^{\alpha/(1-2\alpha)}; \quad (25)$$

this corresponds to the Kolmogorov scale for that event, and depends on the value of α . In particular, events with $\alpha = 3/2$ have the normally defined Kolmogorov scale, while events with $\alpha < 3/2$ have a reduced minimum scale. This expression is similar to those obtained for the Kolmogorov length in the multifractal description of turbulence, where $l_k \sim R^{-1/(1-h)}$ for the Holder exponent h [41].

This fluctuating Kolmogorov scale effects the maximum gradient observed in different events. Assuming that the crossover to viscous dominating times signals the end of the growth of the gradients, one can estimate that

$$(\nabla_i u_j)_k \sim \frac{u^*}{L^*} (R^*)^{1/(2\alpha-1)}, \quad (26)$$

which depends on α . This estimate serves for both strains and vorticity. The crossover acceleration then scales as the maximum value that the inertial term takes

$$a_k \sim \frac{(u^*)^2}{L^*} (R^*)^{(\alpha-2)/(2\alpha-1)}. \quad (27)$$

This leads to a prediction that the index α effects the maximum acceleration in a particular way. In the case $\alpha < 2$, the crossover acceleration a_k shrinks with increasing Reynolds number, while for $\alpha > 2$, the crossover acceleration grows with acceleration. Presumably the viscosity caps the maximum acceleration, but these values still grow without bound with increasing Reynolds number. Note for all of these estimates $\alpha = 1/2$ corresponding to the Leray solution [13] yields an uncapped singularity.

Another way that the maximum gradients may be capped comes about due to the outer solution. As these events must live in a finite domain, and must be patched onto realistic boundary conditions, the ideal form cannot exist out to large radius. Thus either through this departure in the far field, or by the outer condition deviating from the ideal form, the inner solution may miss the maximally focused condition before viscosity would cap the event.

9 Experimental observations

Although the main parts of this paper are analytical, with some turbulent gradient data in hand, I present some limited support for these ideas. A novel optical instrument has been utilized to measure the gradients

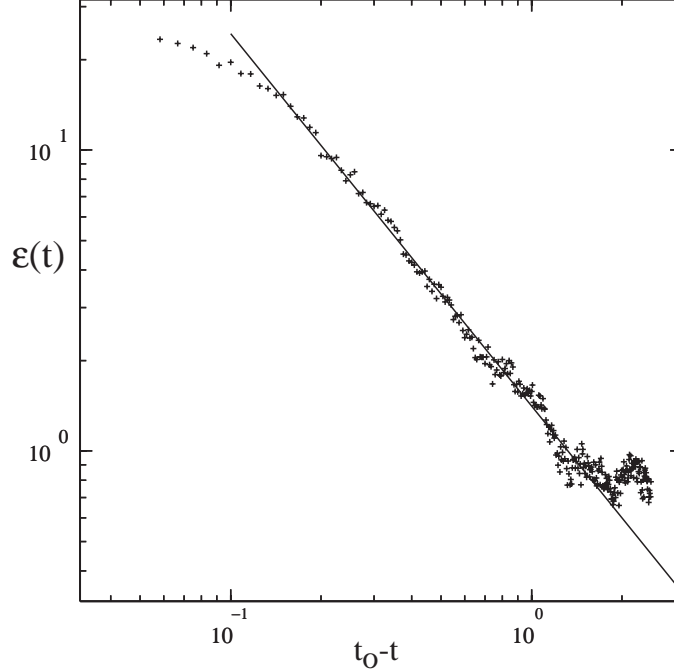


Figure 2: The rise in the dissipation for the event shown in Fig. 1 has a power law form for some range in times. Many such time series are examined to obtain events when the rise is of power law form for at least one decade in time, with a coefficient of regression for this decade of at least $R = 0.98$.

$\partial_i u_j(t)$ at the Kolmogorov scale (see [9] for details about the flow and instrument). Focusing on the most extreme gradient events, I presume that one needs to be both looking at the center of the event and near the critical time in order to have extremely large gradients. Since the measurement is Eulerian, solutions to Eq. 7 will both develop in place, and more probably, be swept by the measurement volume. As these are swept by, the time dependence reflects the spatial dependence of the field; near the critical time this is the far field dependence.

The far field has velocities scaling as $v_i \sim r^{(\alpha-1)/\alpha}$ so that gradients behave as $\partial_i u_j \sim r^{-1/\alpha}$. The dissipation per unit mass $\epsilon = (\nu/2) \sum_{ij} (\partial_i u_j + \partial_j u_i)^2 \sim r^{-2/\alpha}$. Fig. 1 shows one example of a time trace for a large dissipation event. As events are swept by one might occasion to see $\epsilon(t) \sim t^{-2/\alpha}$. An extensive data set of gradients has been examined for events where the dissipation behaves as

$$\epsilon(t) \sim (t_o - t)^\delta \quad (28)$$

for some $t_1 < t < t_2 < t_o$. So that they are at least minimally serious scaling I require at least one decade of scaling, i.e. $(t_1 - t_o)/(t_2 - t_o) = 10$ with a coefficient of regression for a fit to Eq. 28, $R^2 > 0.98$. The event shown in Fig. 1 is redrawn around the large dissipation growth showing (Fig. 2) one example of such a scaling. Figure 3 shows a histogram of the $\alpha = -2/\delta$ values for all 892 events observed of this type. Note that the Kolmogorov value $\alpha = 3/2$ occurs near the observed maxima. These observations are only intended to partially support the analysis discussed as the bulk of this paper. Further experimental testing will be discussed elsewhere so as to not distract from the main points presented here.

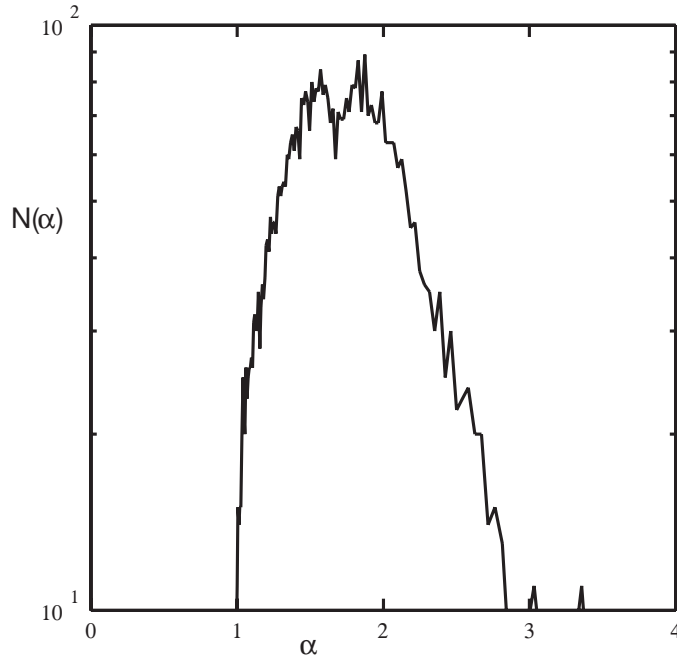


Figure 3: Histogram of the observed values of the exponent α , measured from the rise in dissipation, conditioned as indicated in Fig. 2.

10 Conclusions

The observation of events with $1 \leq \alpha < 3$ may be associated with the much prior commented on multiscaling of the velocity field [16]. The solutions corresponding to K41 statistics is $\alpha = 3/2$. Why these solutions are dominant may be of similar reasons to the Burgers case, where the same exponent also dominates. One might hypothesize that locations where the gradients obey $M + M^2 = \Pi_2$ and the second derivatives $(\partial_i \partial_j v_k)$ vanish may be the locations susceptible to this types of blowup – in analogy to inviscid Burgers shock development. The dominance then of the cubic terms in the velocity near field leads, through a characteristic collapse, to $\alpha = 3/2$ events. While other types of α events also appear possible, a selection mechanism is not obvious.

And then one must deal with the fact that these solutions are self-similar around one point in time and space, while turbulence is a statistically self-affine (or multi-affine) phenomena [8, 16, 10]. What is needed is a number of events associated with Eq. 7 occurring at many spatial locations and times. This may be accommodated if these solutions give rise to the growth of additional events nearby due to the form the intermediate field takes. In particular, if a sufficiently complicated angular structure for the far field occurs, when that must flow into the relatively simple near field, there may be locations with the right type of structure (perhaps in the second order derivative field) which gives rise to new growing collapse events.

Finally, these events are distinct from long lived vortices others have observed, but perhaps causally connected. A sudden growth of the gradients around a point might be expected when two tube-like vortices collide obliquely [42]. Also, I acknowledge that more complicated solutions, perhaps with less trivial length scaling may also play an important role.

Acknowledgements

I would like to greatly acknowledge the support of the National Science Foundation and the Research

Corporation, and stimulating advice from T. Antonsen, J. Gibbon, R.M. Kerr, C.D. Levermore, J. Lister, E. Ott, R. Pego, K.R. Sreenivasan, and E. Tadmor. The experiments could not have been conducted without the efforts and advice of B.W. Zeff, D.D. Lanterman, R. McAllister, R. Roy, and E.J. Kostelich.

References

- [1] G.I. Barenblatt, *Scaling, Self-Similarity and Intermediate Asymptotics* (Cambridge University Press, 1996).
- [2] J.M. Greene and R.B. Pelz, Phys. Rev. E **62**, 7982 (2000), J.M. Greene and O.N. Boratav, Physica **D107**, 57 (1997).
- [3] A.N. Kolmogorov, The local structure of turbulence in the incompressible viscous fluid for very large Reynolds numbers. *Dokl. Akad. Nauk. SSSR* **30**, 301-305 (1941), reprinted in *Proc. R. Soc. Lond. A* **434**, 9-13 (1991).
- [4] A.N. Kolmogorov, Dissipation of energy in the locally isotropic turbulence. *Dokl. Akad. Nauk. SSSR* **31**, 538-540 (1941), reprinted in *Proc. R. Soc. Lond. A* **434**, 15-17 (1991).
- [5] U. Frisch, *Turbulence, the Legacy of A.N. Kolmogorov*, Cambridge Univ. Press (1995).
- [6] A. La Porta, G.A. Voth, A.M. Crawford, J. Alexander, & E. Bodenschatz, Fluid particle accelerations in fully developed turbulence. *Nature* **409**, 1017-1019 (2001).
- [7] N. Mordant, P. Metz, O. Michel, & J.-F. Pinton, Measurement of Lagrangian velocity in fully developed turbulence. *Phys. Rev. Lett.* **87**, 214501-1-4 (2001).
- [8] C. Meneveau & K.R. Sreenivasan, Simple multifractal cascade model for fully developed turbulence. *Phys. Rev. Lett.* **59**, 1424-1427 (1987).
- [9] B.W. Zeff, D.D. Lanterman, R. McAllister, R. Roy, E.J. Kostelich, and D.P. Lathrop, *Nature* **421**, 146 (2003).
- [10] K.R. Sreenivasan and C. Meneveau, Phys. Rev. A **38**, 6287 (1988).
- [11] J.D. Gibbon and C.R. Doering, J. Fluid Mech. **478**, 227 (2003).
- [12] J.M. Burgers, Proc. KNAW **43**, 2 (1940). Reproduced in "Selected Papers of J.M. Burgers," Eds. F.T.M. Nieuwstadt and J.A. Steketee, Kluwer Acad. Pubs. 1995.
- [13] J. Leray, Acta Math. **63**, 193 (1934).
- [14] P. Constantin, SIAM Rev. **36**, 73 (1994).
- [15] R.M. Kerr, Phys. Fluids A **5**, 1725 (1993).
- [16] K.R. Sreenivasan, Fractals and multifractals in fluid turbulence. *Ann. Rev. of Fluid Mech.* **23**, 539-600 (1991).
- [17] J. Eggers, Phys. Rev. Lett. **71**, 3458 (1993), J. Eggers, Rev. Mod. Phys. **69**, 865 (1997).
- [18] D. Leppinen and J.R. Lister, Phys. Fluids **15**, 568 (2003).
- [19] H.A. Stone and J.R. Lister, Phys. Fluids **10**, 2758 (1998).

- [20] M.P. Brenner, J.R. Lister, and H.A. Stone, *Phys. Fluids* **8**, 2827 (1996).
- [21] B.W. Zeff, B. Kleber, J. Fineberg, and D.P. Lathrop, *Nature* **403**, 401 (2000). *Nature* **421**, 146 (2003).
- [22] R.Pego, private communication (2003).
- [23] Weinan E, K. Khanin, A. Mazel, and Y. Sinai, *Phys. Rev. Lett.* **78**, 1904 (1997). J. Bec, *Phys. Rev. Lett.* **87**, 104501 (2001).
- [24] A.J. Majda, & A.L. Bertozzi, *Vorticity and Incompressible Flow* 6-13 (Cambridge Univ. Press, Cambridge, 2002).
- [25] J. Guckenheimer and P. Holmes, *Nonlinear oscillations, dynamical systems, and bifurcations of vector fields*, Springer-Verlag, New York (1983).
- [26] E. Tadmor, private communication, April 2003.
- [27] B.J. Cantwell, *Phys. Fluids A*, **4**, 782 (1992).
- [28] R.B. Pelz and Y. Gulak, *Phys. Rev. Lett.* **79**, 4998 (1997).
- [29] S. Tanveer and C.G. Speziale, *Phys. Fluids A* **5**, 1456 (1993).
- [30] L. Tuckerman, private communication, 2003.
- [31] J.D. Gibbon, *Physica D* **166**, 17 (2002).
- [32] J. Necas, M. Ruzicka, and V. Sverak, *Acta Math.* **176**, 283 (1996).
- [33] C. Uhlig and J. Eggers, *Z. Phys. B* **103**, 69 (1997).
- [34] E.D. Siggia and A. Pumir, *Phys. Rev. Lett.* **55**, 1749 (1985).
- [35] A. La Porta, G.A. Voth, F. Moisy, and E. Bodenschatz, *Phys. of Fluids* **12**, 1485 (2000).
- [36] R.B. Pelz, *Phys. Rev. E* **55**, 1617 (1997).
- [37] A. Pumir and E. Siggia, *Phys. Fluids A* **2**, 220 (1990).
- [38] M.E. Brachet, M. Meneguzzi, A. Vincent, H. Politano, and P.L. Sulem, *Phys. Fluids A* **4**, 2845 (1992).
- [39] K. Ohkitani, *Phys. Fluids A* **5**, 2570 (1993).
- [40] S. Kida & K. Ohkitani, Spatiotemporal intermittency and instability of a forced turbulence. *Phys. Fluids A* **4**, 1018-1027 (1992).
- [41] T. Bohr, M.H. Jensen, G. Paladin, and A. Vulpiani, *Dynamical Systems Approach to Turbulence*, Cambridge Univ. Press (1998).
- [42] R. Kerr, private communication (2002).